Cancer Letters 449 (2019) 252–262

Contents lists available at ScienceDirect

Cancer Letters

journal homepage: www.elsevier.com/locate/canlet

Original Articles

Proton pump inhibitors promote the growth of androgen-sensitive prostate cancer cells through ErbB2, ERK1/2, PI3K/Akt, GSK-3β signaling and inhibition of cellular prostatic acid phosphatase

Iacopo Gesmundo[a], Laura Di Blasio[b,c], Dana Banfi[a], Tania Villanova[a], Alessandro Fanciulli[a], Enrica Favaro[a], Giacomo Gamba[a], Chiara Musuraca[c,d], Ida Rapa[e], Marco Volante[e], Stefania Munegato[f], Mauro Papotti[c,d], Paolo Gontero[f], Luca Primo[b,c], Ezio Ghigo[a,1], Riccarda Granata[a,*,1]

[a] Division of Endocrinology, Diabetes and Metabolism, Department of Medical Sciences, University of Turin and Città Della Salute e Della Scienza Hospital, Turin, 10126, Italy
[b] Candiolo Cancer Institute FPO-IRCCS, Candiolo, Turin, 10060, Italy
[c] Department of Oncology, University of Turin, Turin, Italy
[d] Città Della Salute e Della Scienza Hospital, Turin, 10126, Italy
[e] Department of Oncology, University of Turin, San Luigi Hospital, Orbassano, Turin, 10043, Italy
[f] Division of Urology, Department of Surgical Sciences, University of Turin and Città Della Salute e Della Scienza Hospital, Turin, 10126, Italy

ARTICLE INFO

Keywords:
Proton pump inhibitors
Prostate cancer cells
Primary prostate epithelial cells
Prostate specific antigen
Cellular prostatic acid phosphatase

ABSTRACT

Prostate cancer (PCa) is one of the most common cancer in men. Although hormone-sensitive PCa responds to androgen-deprivation, there are no effective therapies for castration-resistant PCa. It has been recently suggested that proton pump inhibitors (PPIs) may increase the risk of certain cancers; however, association with PCa remains elusive. Here, we evaluated the tumorigenic activities of PPIs *in vitro*, in PCa cell lines and epithelial cells from benign prostatic hyperplasia (BPH) and *in vivo*, in PCa mice xenografts. PPIs increased survival and proliferation, and inhibited apoptosis in LNCaP cells. These effects were attenuated or absent in androgen-insensitive DU-145 and PC3 cells, respectively. Specifically, omeprazole (OME) promoted cell cycle progression, increased c-Myc expression, ErbB2 activity and PSA secretion. Furthermore, OME induced the phosphorylation of MAPK-ERK1/2, PI3K/Akt and GSK-3β, and blunted the expression and activity of cellular prostatic acid phosphatase. OME also increased survival, proliferation and PSA levels in BPH cells. *In vivo*, OME promoted tumor growth in mice bearing LNCaP xenografts. Our results indicate that PPIs display tumorigenic activities in PCa cells, suggesting that their long-term administration in patients should be carefully monitored.

1. Introduction

Prostate cancer (PCa) is the second leading cause of cancer death in men in industrialized countries [1]. Androgens and androgen receptor (AR) signaling are essential to PCa development and progression, and androgen deprivation therapy (ADT) is considered as the first line

Abbreviations: ADT, androgen deprivation therapy; AR, androgen receptor; Bcl-2, B-cell lymphoma-2; BPH, benign prostatic hyperplasia; BME, basement extract; BrdU, 5-bromo-2-deoxyuridine; BSA, bovine serum albumin; CGA, chromogranin A; cPAcP, cellular prostatic acid phosphatase; CRPC, castration-resistant prostate cancer; DMEM, Dulbecco's Modified Eagle's medium; DTX, docetaxel; EDTA, ethylenediaminetetraacetic acid; ELISA, enzyme-linked immunosorbent assay; ErbB2, erythroblastic leukemia viral oncogene homolog 2; ERK1/2, extracellular signal-regulated protein kinases 1 and 2; ESO, esomeprazole; GSK-3β, glycogen synthase kinase-3 beta; LAN, lansoprazole; mTOR, mammalian target of rapamycin; MTT, 3-(4,5-Dimethylthiazol-2-yl)-2,5-diphenyltetrazolium bromide; OME, omeprazole; PBS, phosphate-buffered saline; PCa, prostate cancer; PI3K, phosphatidylinositol 3 kinase; PPIs, proton pump inhibitors; PTEN, phosphatase and tensin homolog; PSA, prostate-specific antigen; SCID, severe combined immunodeficient; RT-PCR, reverse transcriptase-polymerase chain reaction; TURP, transurethral resection of prostate

* Corresponding author. Division of Endocrinology, Diabetes and Metabolism, Department of Medical Science, University of Turin and Città della Salute e della Scienza Hospital, Corso Dogliotti, 14, 10126, Turin, Italy.
E-mail address: riccarda.granata@unito.it (R. Granata).
[1] The Authors contributed equally to the study.

https://doi.org/10.1016/j.canlet.2019.02.028
Received 23 November 2018; Received in revised form 8 February 2019; Accepted 14 February 2019
0304-3835/ © 2019 Elsevier B.V. All rights reserved.

therapy for advanced PCa. However, although most patients with PCa show an initial response to ADT, the majority eventually progress to a castration-resistant state, the management of which remains a substantial challenge [2,3].

In addition to the AR signaling axis, different pathways have been shown to be dysregulated in patients with PCa. These include the phosphoinositide 3-kinase (PI3K)/Akt-mammalian target of rapamycin (mTOR), hyperactivated in response to the loss of phosphatase and tensin homolog (PTEN), and mitogen-activated protein kinase (MAPK), frequently activated in PCa because of perturbation of *Ras* or *Raf* signaling [2,3]. Furthermore, overexpression and activation of receptor tyrosine kinases, including ErbB-2 (Her-2/neu), were found to enhance the stability and activity of AR in castration-resistant PCa (CRPC) [4]. Thus, understanding the molecular mechanisms involved in androgen independence would lead to the identification of new therapeutic approaches for combating PCa.

Proton pump inhibitors (PPIs) are among the most commonly used drugs in the world for gastroesophageal reflux disease (GERD) and peptic ulcer disease. Omeprazole (OME), the first drug in this class, was introduced in 1989, followed by others such as lansoprazole (LAN) and esomeprazole (ESO). PPIs inhibit gastric acid secretion by irreversibly binding to the hydrogen/potassium ATPase enzyme in gastric parietal cells and are the treatment of choice of acid-related diseases [5]. Although generally considered safe, in the past decade there have been increasing concerns on the adverse effects and complications of the long-term use of PPIs, which included increased risk in hip fracture, adverse cardiovascular events and chronic kidney disease [6,7]. Regarding the effects in cancer, PPIs have been found to display antitumor action, both alone and in combination with chemotherapeutic agents [8,9]. However, recent studies have also shown an association between long-term use of PPIs and increased risk in gastric cancer [10–12], colorectal cancer [13] and pancreatic cancer [14]. In animals, it was reported that OME promotes carcinogenesis in rat liver [15] and in forestomach in mice [16]. Moreover, long-term administration of OME worsened atrophic corpus gastritis and induced the development of adenocarcinoma in Mongolian gerbils [17].

With regard to the effects of PPIs in the prostate, a recent study reported that PPI intake elevated the levels of chromogranin A (CGA) in patients with chemotherapy-naïve CRPC [18]; moreover, both short- and long-term use of PPIs increased the levels of CGA in man [19,20]. Interestingly, in addition to being a key biomarker for the diagnosis and follow-up of neuroendocrine tumors [21], it has been recently suggested that elevated levels of CGA are associated with reduced overall survival in metastatic CRPC [22].

Based on the foregoing, the present study aimed to assess the role, if any, of PPIs in PCa. The effects of PPIs, specifically of OME, were assessed on cell survival, proliferation and apoptosis, along with the mechanisms, in PCa cell lines and human primary prostate epithelial cells from benign prostatic hyperplasia (BPH). Furthermore, the effect of OME on tumor growth was determined *in vivo* in mice bearing LNCaP tumor xenografts.

2. Materials and methods

2.1. Reagents

Omeprazole (OME), lansoprazole (LAN), esomeprazole (ESO), docetaxel (DTX), 3-[4,5-dimethylthiazol-2-yl], 2,5-diphenyl tetrazolium bromide (MTT), Roswell Park Memorial Institute (RPMI)-1640 medium, Dulbecco's Modified Eagle's medium (DMEM), DMEM/F12, fetal bovine serum (FBS), bovine serum albumin (BSA), penicillin, streptomycin, amphotericin B, primers for RT-PCR, PD98059, LY-294002, and cell culture reagents were from Sigma-Aldrich (Milan, Italy). Rabbit polyclonal antibodies for phosphorylated (P)-Akt (Ser 473), P-glycogen synthase kinase-3 beta (GSK-3β) (Ser9), P-ERK1/2 and cellular prostatic acid phosphatase (cPAcP) were from Cell Signaling Technology (Euroclone SpA, Milan, Italy). c-Myc, Bcl-2 and actin antibodies were from Santa Cruz Biotechnology (Heidelberg, Germany). RT-PCR and Real-Time PCR reagents were from Life Technologies, Inc. (Invitrogen, Milan, Italy).

2.2. Cell culture

LNCaP, DU145 and PC3 human PCa cells; MSTO-211H human malignant biphasic pleural mesothelioma cells; MCF-7 and SK-BR-3 human breast cancer cells; N-87 human gastric carcinoma cells; T HESCs human endometrium non-malignant myomas; HT-29 human colon adenocarcinoma cells; HeLa human cervix adenocarcinoma cells; HepG-2 human liver carcinoma cells; Jurkat human T-cell leukemia; MeT-5A human mesothelial cells; AtT-20/D16v-F2 murine pituitary tumor cells; C2C12 murine myoblasts; H9C2 rat cardiac cells and 3T3-L1 murine pre-adipocytes were obtained from the American Type Culture Collection (Manassas, VA, USA). INS-1E cells rat insulinoma were purchased from AddexBio (San Diego, CA, USA). REN human malignant epithelial pleural mesothelioma cells were kindly provided by Prof. Giorgio Scagliotti (Department of Oncology, University of Turin, San Luigi Hospital, Orbassano, Turin, Italy). LNCaP, MSTO-211H, SK-BR-3, HT-29, HeLA, HepG-2, Jurkat, Met-5A, AtT-20/D16v-F2, INS-1E and REN cells were maintained in medium RPMI 1640 supplemented with 10% FBS. DU145, PC3, MCF-7, N-87, C2C12, H9C2 and 3T3-L1 cells were maintained in DMEM supplemented with 10% FBS. T HESCs were cultured in DMEM/F12 with 10% FBS. All culture media were supplemented with L-glutamine (2 mM), penicillin (100 U/ml), streptomycin (100 µg/ml) and 250 ng/ml amphotericin B. The cells were cultured at 37 °C in a 5% CO_2 humidified atmosphere.

2.3. Isolation of human primary prostate cells from benign prostatic hyperplasia (BPH)

Prostate tissue was obtained from transurethral resection of prostate (TURP) surgery of individuals with benign prostatic hyperplasia (BPH), who had given informed consent before surgery. The study protocol was approved by the Local Committee of A.O.U. Città della Salute e della Scienza di Torino - A.O. Ordine Mauriziano – A.S.L. Città di Torino (N. 0026342). Fresh prostate specimens were rinsed to remove blood cells, mechanically minced into small pieces and enzymatically digested in DMEM containing type I collagenase (2 mg/ml) for 2 h at 37 °C. The dissociated cell suspension was then passed through a 70 µm pre-separation filter and centrifuged at 2000 rpm for 5 min. The cells, resuspended in complete medium and plated on 6-well plates, were maintained in DMEM with 10% FBS, 100 U/mL penicillin, 100 µg/mL streptomycin, 250 ng/mL amphotericin B and epidermal growth factor (EGF) (10 ng/mL) and cultured in a humidified atmosphere at 37 °C in 5% CO_2. Expression of prostate-specific antigen (PSA) as prostate marker was used to confirm the prostatic origin of the cells.

2.4. Cell survival and proliferation

The cells were seeded in 96-well plates at 3×10^3 cells/well and cultured for 48, then serum-starved for 12 h and incubated with the different stimuli for further 24 h or 48 h. Cell survival and proliferation were assessed by MTT and 5-bromo-2-deoxyuridine (BrdU) incorporation ELISA kit (Roche Diagnostic SPA, Milan, Italy), respectively, as previously described [23]. Absorbance was assessed by spectrophotometry at 570 nm for MTT and at 450 nm for BrdU, using LT-4000 microplate reader (Euroclone, Milan, Italy).

2.5. Caspase-3 activity

Cells were seeded in 6-well plates at a concentration of 5×10^4 cells/well. Caspase-3 activity was assessed by Caspase-3 Colorimetric Assay Kit (BioVision, USA) in cell lysates, according to the

manufacturer's instruction and analyzed by colorimetric detection at 450 nm absorbance with a LT-4000 microplate reader (Euroclone, Milan, Italy).

2.6. Immunostaining on LNCaP cells

The cells were scraped, collected and centrifuged for 5 min at 800 rpm. Cell pellets were rinsed twice in phosphate buffer saline solution (PBS 1X), fixed in 4% neutral-buffered formalin at room temperature for 20 min, routinely processed to paraffin embedding with an automatic processor (Leica ASP 300, Leica Microsystems, Wetzlar, Germany) and embedded in paraffin wax. 3 μm-thick sections were cut for immunohistochemistry (IHC). IHC was performed using an automated slide-processing platform (Ventana BenchMark XT AutoStainer, Ventana Medical Systems, Tucson, AZ, USA) with the following primary antibody: anti-Androgen Receptor Rabbit Monoclonal Antibody (SP107, Ventana Medical Systems). Positive (human prostate tissue) and negative (omission of the primary antibody) controls were included for each immunohistochemical run. Images were acquired with the Hamamatsu NanoZoomer S210 scanner by Nikon.

2.7. PSA secretion

LNCaP cells were seeded in 24-well plates (1×10^4 cells/well) and primary BPH cells were seeded in 6-well plates (5×10^4 cells/well). After 48 h the cells were serum starved overnight and incubated with OME at the indicated concentrations for further 24 h. Cell conditioned medium was collected and total PSA secretion assessed by colorimetric assay at 450 nm absorbance using Total PSA Elisa kit (NovaTec, Dietzenbach, Germany), following the manufacturer's instructions.

2.8. cPAcP activity

LNCaP cells were seeded (5×10^4) in 60-mm plates for 48 h, serum-starved for 12 h and incubated for 24 h with OME. The cells were then homogenized, centrifuged (13,000 rpm for 3 min) and cPAcP activity was measured with Acid Phosphatase Assay Kit (Abcam,UK) following the manufacturer's instructions and by colorimetric detection at 450 nm.

2.9. HER2/ErbB2 phosphorylation

LNCaP cells were seeded (2×10^5) in 100-mm dishes. After 48 h the cells were serum-starved for 12 h and treated with 1 μM OME for 12 and 24 h. Briefly, the cells were homogenized, sonicated and centrifuged to remove insoluble material (14,000 rpm for 10 min) and the phosphorylation of HER2/ErbB2 on Tyr1221/1222 was assessed with the PathScan Phospho-HER2/ErbB2 Sandwich ELISA Kit (Cell Signaling Technology, Euroclone, Milan, Italy) following the manufacturer's instructions and detected at 450 nm.

2.10. Cell cycle analysis

Cell cycle analysis was performed using the Muse Cell Cycle Kit (Merck-Millipore, USA) according to the manufacturer's instructions. Briefly, 5×10^4 cells were seeded in 60-mm dishes and after 48 h incubated with OME in medium supplemented with 2.5% FBS for 24 h. Cells were then detached with PBS 1X/EDTA (5 mM), centrifuged (1500 rpm, 5 min) and fixed with pre-cooled ethanol. The cells were then treated with Muse Cell Cycle Reagent for 30 min and analyzed with Muse Cell Analyzer Software (Merck Millipore, USA).

2.11. Colony formation

LNCaP cells were seeded into 60-mm plates, at 1500 cells/plate, and cultured for 12 days in either presence or absence of OME. The cells were then fixed with methanol, colonies stained with crystal violet (0.05%) and plates photographed using a digital camera. Colonies were counted with Image J software (https://imagej.nih.gov).

2.12. Real-Time PCR

Total RNA extraction and reverse transcription to cDNA (1 μg RNA) from LNCaP were performed as previously described [24]. Real-time PCR was performed with 50 ng cDNA, 100 nmol/L of each primer and the IQ-SYBR-green Mastermix (Bio-Rad, Milano, Italy) using the ABI-Prism 7300 (Applied Biosystems). The following primer pairs were used: cPAcP, forward 5′-GCCGTATCCCCTCATGCTAC-3′, reverse 5′-CAGCTCAGCAAACCTCTCCA-3' (NM_001292037.1); AR, forward 5′-AGCAAGAGACTAGCCCCAGG-3′, reverse 5′-CTACGATGGGCTTGGCGAGA-3' (NM_001348064.1); c-Myc, forward 5′-AGCGACTCTGAGGAGGAACA -3′, reverse 5′-CTCTGACCTTTTGCCAGGAG-3' (NM_002467.5); cyclin-A forward 5′-AATTGTGCCTTGCCTGAGTGA-3′, reverse 5′-AAGAACTGCAGGTGGCTCCAT-3' (XM_011535295.2); cyclin-B1 forward 5′-CGAAGATCAACATGGCAGG-3′, reverse 5′-CTTGGAGAGGCAGTATCAACC-3' (NM_001354844.1); 18s rRNA. forward 5′-CCCATTCGAACGTCTGCCCTATC-3′, reverse 5′-TGCTGCCTTCCTTGGATGTGGTA-3' (NR_146144.1). 18s rRNA was used as endogenous control. Relative quantification was performed using the comparative Ct ($2-\Delta\Delta Ct$) method.

2.13. Western blot analysis

Immunoblot analysis was performed as described previously [25]. Protein immunoprecipitation with Protein A Sepharose beads (Sigma-Aldrich, Milan, Italy) was performed for detection following the manufacturer's instructions. Proteins were resolved in 10% SDS-PAGE (12% for Bcl-2) and transferred to a nitrocellulose membrane; after blocking with 1% BSA in Tris-buffered saline with 0.1% Tween for 2 h at room temperature, membranes were incubated overnight at 4 °C with the specific antibody (P-ERK1/2, P-AKT, P-GSK-3β, c-Myc, Bcl-2, cPAcP and actin) (dilution 1:1000, actin, c-Myc and Bcl-2 1:500). Blots were reprobed with the respective total antibodies or actin for normalization. Immunoreactive proteins were visualized using horseradish peroxidase-conjugated goat anti-mouse or goat anti-rabbit (1:4000) antibodies by enhanced chemiluminescence using ChemiDoc XRS (Bio-Rad, Milan, Italy). Densitometric analysis was performed with Quantity One software (Bio-Rad, Segrate, Milan, Italy).

2.14. 3D cell culture

3D cell culture of LNCaP cells was performed as described previously [26]. Briefly, 2×10^3 cells were seeded in a basement membrane extract (BME) gel. After polymerization, each well was filled with 500 μl DMEM with 10% FBS, with or without 1 μM OME. The media were replaced every two days. Cells were imaged at different time points (0, 8, 10, 13 days) and the diameter of the colonies was measured after 13 days using Image J Software (https://imagej.nih.gov).

2.15. In vivo tumor growth

All animal procedures were performed according to institutional guidelines in compliance with national (D.L. N.26, 04/03/2014) and international law and policies (new directive 2010/63/EU). The protocol was approved by the Italian Ministry of Health (n.1073/2015-PR). 8-week-old male NOD (non-obese diabetic)/SCID (severe combined immunodeficient) were housed and bred at Candiolo Cancer Institute IRCCS, Candiolo, Turin, Italy. The mice were injected subcutaneously in both flanks with 3×10^6 LNCaP cells in 200 μl of 1:1 culture medium:Matrigel solution. When tumors became evident, about 1 week after injection, the mice were randomly divided into two groups, Control and OME (6 mice each group). OME (dissolved in water) was

administered at a dose of 7.2 mg/kg by oral gavage every two days for 7 weeks. As previously reported, this is considered as a low dose, based on long-term clinical administration in humans [16]. Mice from the Control group received vehicle solution. Tumor measurements were performed once a week, from week 4 until the end of the experiment (week 7). Animals were sacrificed at the end of the treatments and tumors explanted for subsequent analysis. Tumor volume from each flank was calculated with the formula $v = (a \times b^2)/2$, where a is the long axis and b is the short axis. Tumors were resected and fixed in 4% v/v paraformaldehyde. Paraffin sections were stained with hematoxylin/eosin (H/E) for immunohistochemistry analysis. Standard immunoperoxidase analysis was performed for PSA using a polyclonal rabbit anti-PSA antibody (1:200, AgilentDako, Santa Clara, USA) and a biotin-free detection system (EnVision™Plus, AgilentDako, Santa Clara, USA).

2.16. Statistical analysis

Results are presented as mean ± SEM. Significance was calculated by two-tailed Student's *t*-test or two-way ANOVA followed by Bonferroni's multiple comparison test for post hoc analysis. Analysis was performed using GraphPad Prism 5.0. Significance was established for $P < 0.05$.

3. Results

3.1. PPIs promote survival and proliferation, and inhibit apoptosis in LNCaP PCa cells

The role of OME, LAN and ESO was first assessed on survival, proliferation and apoptosis in androgen-sensitive LNCaP cells. Serum-starved cells were treated for 24 h with increasing concentrations of each PPI (0.1–2 μM). Cell survival and proliferation were evaluated by MTT and BrdU assays, respectively, and apoptosis by activation of caspase-3. As expected, cell proliferation and survival were reduced under serum starvation (control), compared with normal medium. OME dose-dependently increased cell survival and proliferation as compared with untreated cells (control), showing the strongest effect at 1 and 2 μM (Fig. 1A and B). Similar results were obtained at 48 h, where OME increased cell survival and proliferation at 1 and 2 μM and at 0.5–2 μM, respectively (Figs. S1A and B). Furthermore, at 24 h OME reduced apoptosis to levels comparable with those of normal medium (Fig. 1C); conversely, cell survival and growth were unchanged in cells treated with OME in normal medium (Figs. S1C and D). Similar results were observed for LAN, which increased cell survival at 1 and 2 μM (Fig. 1D), proliferation at 0.5–2 μM (Fig. 1E), and reduced apoptosis at 0.5–2 μM (Fig. 1F). ESO exerted the same dose-dependent actions (from 0.5 μM) (Fig. 1G–I).

The role of OME was next assessed on the response to Docetaxel (DTX), a taxan agent and one of the major chemotherapy compounds for treatment of CRPC [27]. Following the previous results, 1 μM OME was selected as the best concentration for subsequent experiments. The cells were initially exposed for 24 h to increasing concentrations of DTX alone, which showed a cytotoxic action at 0.01 μM (Fig. 1J). In cells treated with both OME and DTX we found that OME alone increased, whereas DTX (0.01 μM) reduced cell survival and proliferation, as expected; however, in cells pre-incubated with OME, the inhibitory effects of DTX were blunted, compared with those of DTX alone (Fig. 1K and L).

Overall, these results indicate that PPIs exert survival, proliferative and antiapoptotic effects in LNCaP cells and attenuate the cytotoxic action of chemotherapy drugs.

3.2. The effects of PPIs are reduced or absent in androgen-insensitive DU145 and PC3 PCa cells

The role of OME, LAN and ESO was next tested in DU145 and PC3 cells. After 24 h OME increased cell survival and proliferation only at 2 μM in DU145 cells, (Fig. 2A and B), whereas no effect was observed in PC3 cells, at any of the concentrations tested (Fig. 2C and D). Similarly, LAN and ESO increased cell survival and proliferation in DU145 only at the highest concentrations tested, but displayed no effect in PC3 cells (Additional File 2: Fig. S2).

The role of OME was also analyzed on survival of different human and murine cancer cell lines and non-malignant cells. We found that OME was unable to modify cell survival in any of the cell types tested, suggesting that the effects are limited to PCa cell lines (Table 1).

3.3. OME promotes the progression of cell cycle and expression of c-Myc and Bcl-2 in LNCaP cells

We subsequently verified, through flow cytometry analysis, whether OME-induced proliferation of LNCaP cells was associated with variations in cell cycle. Treatment with OME for 24 h reduced the percentage of cells in G0/G1 phase and increased those in S and G2/M, compared with control (Fig. 3A). Accordingly, expression of *cyclin A* and *cyclin B1*, both associated with progression of cell cycle, was upregulated (Fig. 3B and C). OME also enhanced the expression of the oncoprotein c-Myc and antiapoptotic protein Bcl-2, at both 12 and 24 h, consistent with the previously observed proliferative and antiapoptotic effects (Fig. 3D and E). Moreover, the number of colonies was increased in cells treated for 10 days with 1 μM, and even more with 2 μM OME, compared with untreated (Fig. 3F). The effect of OME was also assessed on the growth on 3D of cell spheroids. LNCaP cells embedded in BME and treated with OME for 8, 10 and 13 days showed an increase in the diameter of spheroids (Fig. 3G).

3.4. OME promotes the phosphorylation of ErbB-2 and secretion of PSA, regulates survival and proliferative pathways and reduces expression and activity of cPAcP in LNCaP cells

We next sought to determine whether OME regulates the expression of AR in LNCaP cells. The mRNA levels of *AR* were not changed after treatment for 24 h with different concentrations of OME (Fig. 4A). Similarly, staining for AR protein showed no variation between cells treated with OME (Fig. 4B, d) and untreated (Fig. 4B and c). Still, OME promoted the phosphorylation of ErbB2 on tyrosine 1221 (Fig. 4C), which has been shown to be associated with elevation in PSA secretion, phosphorylation of MAPK, and reduction in cPAP, along with PCa progression [4,28]. Accordingly, treatment with increasing concentrations of OME for 24 h progressively increased the secretion of PSA, whose levels have been previously shown to be elevated in PCa, as well as in benign prostatic hyperplasia (BPH) [29] (Fig. 4D). Moreover, OME time-dependently promoted the phosphorylation of MAPK ERK1/2 (Fig. 4E), PI3K/Akt (Fig. 4F), and inactivation, i.e. increased phosphorylation, of its downstream effector glycogen synthase kinase 3 beta (GSK-3β) (Fig. 4G), which are all associated with PCa cell proliferation, tumor progression and metastasis [3,30]. The specific inhibitors of ERK1/2 (PD98059) and PI3K/Akt (LY294002) blocked the survival and proliferative activities of OME, whereas no effect was observed using these compounds alone (Fig. 4H–K). OME also reduced both expression and activity of the prostate-specific tumor suppressor cPAcP (Fig. 4L and M), whose inhibition has been associated with increase in ErbB-2 phosphorylation, PCa cell growth and tumor progression [31–33]. Because cPAcP inversely correlates with the growth of PCa cells, we analyzed the presence of cPAcP in LNCaP, PC3 and DU145 cell lines. cPAcP was detected in LNCaP, but not in PC3 and DU145 cells (Fig. 4N), which display higher growth rate compared to LNCaP [34]. Overall, these results suggest that OME promotes survival and

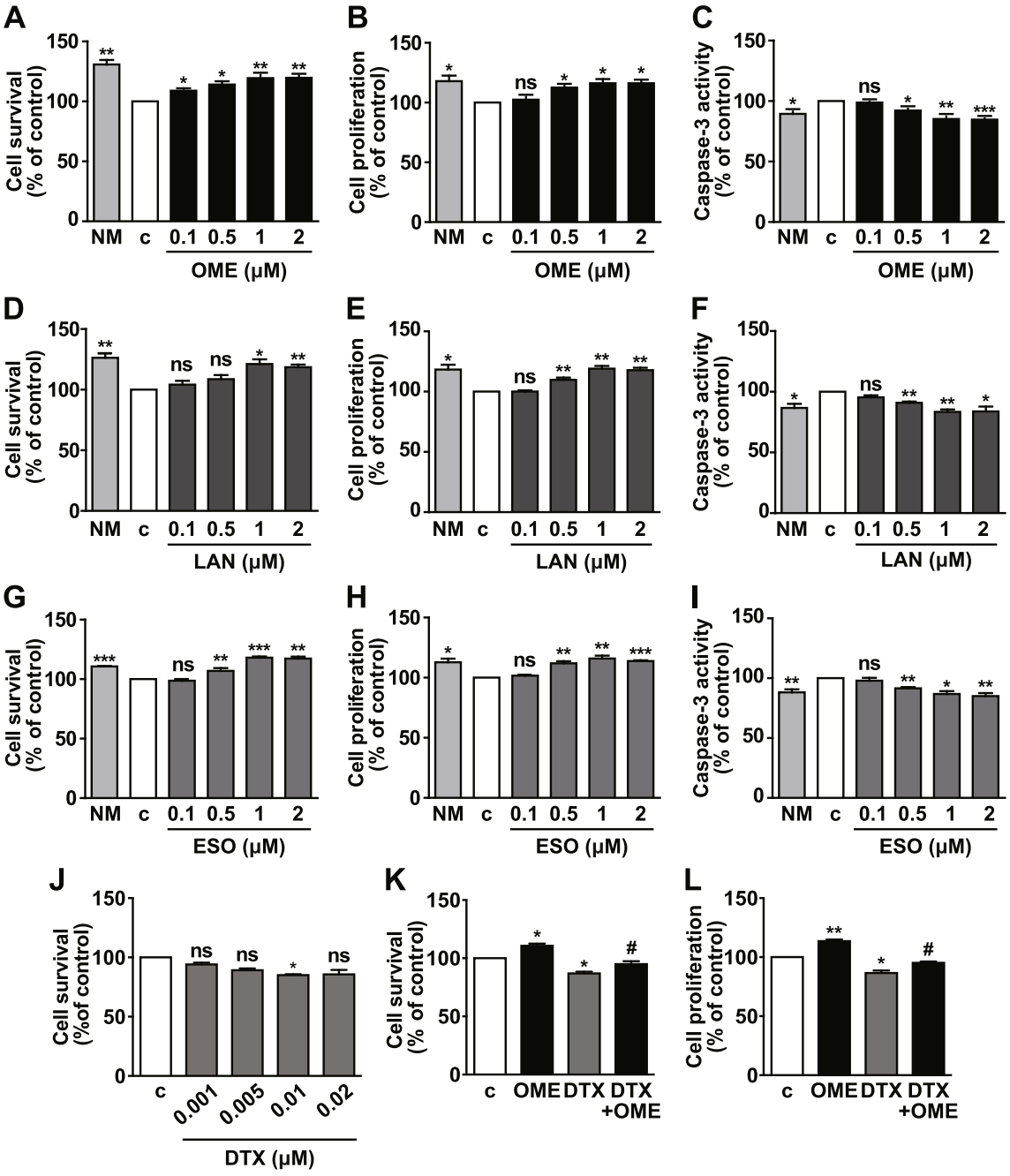

Fig. 1. Effect of PPIs on survival, proliferation and apoptosis of LNCaP cells. The cells were cultured in either normal medium (NM) or in serum-deprived medium (c, control medium) for 12 h, then for further 24 h with OME (A–C), LAN (D–F) or ESO (G–I) at the concentrations indicated. Cell survival and proliferation were assessed by MTT and BrdU assays, respectively, apoptosis as activation of caspase-3. J, Cell survival in cells cultured for 24 h with the indicated concentrations of Docetaxel (DTX). Cell survival (K) and proliferation (L) in cells cultured with either 1 μM OME or 0.01 μM DTX, alone or in combination. Results are expressed as percent of control and are mean ± SEM of three replicates (n = 3). $^{*}P < 0.05$, $^{**}P < 0.01$ and $^{***}P < 0.001$ vs. c; ns, not significant; $^{\#}P < 0.05$ vs. DTX.

proliferation in LNCaP cells through the regulation of pathways involved in PCa growth and progression.

3.5. OME promotes survival and proliferation, and increases PSA in human primary prostate epithelial cells from BPH

BPH is an age-dependent condition, characterized by an enlargement of the prostate due to the expansion of epithelial and stromal cells. BPH may lead to compression of the urethra, resulting in various symptoms, known as lower urinary tract symptoms (LUTSs), for which new therapeutic targets continue to be explored [35]. Thus, based on our results in PCa cells, we next investigated the effect of OME in epithelial cells obtained from human BPH tissue. OME, at increasing concentrations (0.1–2 μM), enhanced cell survival and proliferation, with a maximum effect at 1 μM (Fig. 5A and B), and raised PSA secretion at 1 and 2 μM (Fig. 5C) in BPH cells, that also expressed cPAcP (Fig. 5D). These findings suggest that OME elicits similar functions in both PCa cell lines and primary BPH cells, along with increase in PSA secretion.

3.6. OME promotes tumor growth in a murine xenograft model of PCa

The *in vivo* effect of OME on tumor growth was assessed in NOD/SCID mice bearing LNCaP xenografts. OME was orally administered

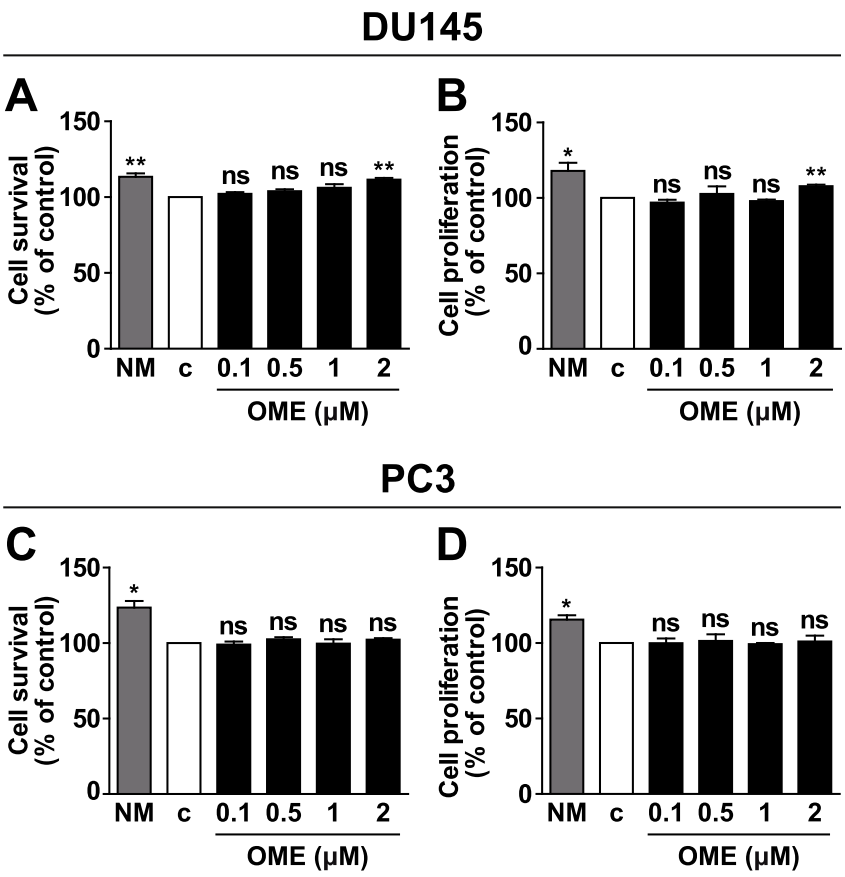

Fig. 2. Effect of OME on survival and proliferation of DU145 and PC3 cells. Serum-starved DU145 (A and B) and PC3 cells (C and D) were cultured for 24 h with the indicated concentrations of OME. Cell survival and proliferation were assessed by MTT and BrdU assays, respectively. Results are expressed as percent of control and reported as mean ± SEM of three replicates (n = 3). $^{*}P < 0.05$ and $^{**}P < 0.01$ vs. c; ns, not significant.

Table 1
Cell survival after treatment with OME (1 μM) for 24 h.

Cell line	Description	Cell survival (% of control)
MSTO-211H	Human malignant mesothelioma biphasic	99.4%
REN	Human malignant mesothelioma epithelioid	102.3%
MCF-7	Human breast adenocarcinoma	100.1%
N87	Human gastric carcinoma	100.7%
T HESCs	Human endometrial stromal cells	96.3%
SK-BR-3	Human breast adenocarcinoma	99.4%
HT-29	Human colon adenocarcinoma	98%
HeLa	Human cervix adenocarcinoma	99%
HepG-2	Human liver carcinoma	101%
Jurkat	Human T-cell leukemia	96%
MeT-5A	Human pleural mesothelial	100.8%
AtT-20/D16v-F	Mouse ACTH-secreting pituitary tumor	102.9%
INS-1E	Rat insulinoma	100.7%
C2C12	Mouse myoblast	100.3%
H9C2	Rat heart myoblast	102.1%
3T3-L1	Mouse preadipocyte	97.8%

every two days for 7 weeks, the mice were sacrificed at the end of the study and the whole tumor tissues were obtained. OME exhibited a remarkable effect on tumor growth, that was increased from week 4 compared with the control group, suggesting a role for OME in promoting tumor progression. The effect was maintained at every week and was significant at week 7, where the average tumor size was 167 mm^3 in mice treated with OME and 39 mm^3 in control mice ($^{*}P < 0.05$) (Fig. 6A). There were no significant differences in body weight among the groups (data not shown). Furthermore, immunohistochemistry analysis showed slightly increased immunoreactivity for PSA in OME group compared with control (Fig. 6B). These results indicate that OME effectively promotes the growth of androgen-sensitive PCa *in vivo*.

4. Discussion

Our results show that PPIs exert survival, proliferative and antiapoptotic effects in PCa cell lines, specifically in androgen-sensitive LNCaP cells. Focusing on OME, we found that the mechanisms included induction of cell cycle progression, increase in expression of oncoproteins such as c-Myc, and reduction of antiapoptotic proteins. Furthermore, OME promoted the phosphorylation of ErbB2 and secretion of PSA, the activation of survival and proliferative pathways, along with inhibition of prostate phosphatases. OME displayed similar survival and proliferative effects in human epithelial prostate cells isolated from patients with BPH; moreover, *in vivo* OME promoted the growth of LNCaP tumor xenografts in mice.

We show here that OME, LAN and ESO elicited similar survival, proliferative and antiapoptotic effects in LNCaP cell; thus, OME was chosen as compound to be tested in the rest of the study. Interestingly, OME also blunted the inhibitory action of DTX in LNCaP cells, suggesting that, at least in androgen-dependent cells, PPIs may alter the sensitivity to DTX, the major taxan agent used for the treatment of PCa [27]. Moreover, despite the fact that no significant effects were observed in DU145 and PC3 androgen-independent cells, it will be important to examine in the future the possible interaction between OME and DTX in CRPC cells.

Noteworthily, OME reduced the G0/G1 phase in LNCaP cells and increased the number of cells in S and G2/M phase, indicating inhibition of cell cycle arrest and induction of cell cycle progression. Consistently, OME also elevated the expression of cyclin A and B1, key regulatory proteins in driving G2 to M phase [36], and of cMyc, which has been associated to the development of PCa and whose levels, elevated in both androgen-sensitive PCa and CRPC, are regulated by AR in

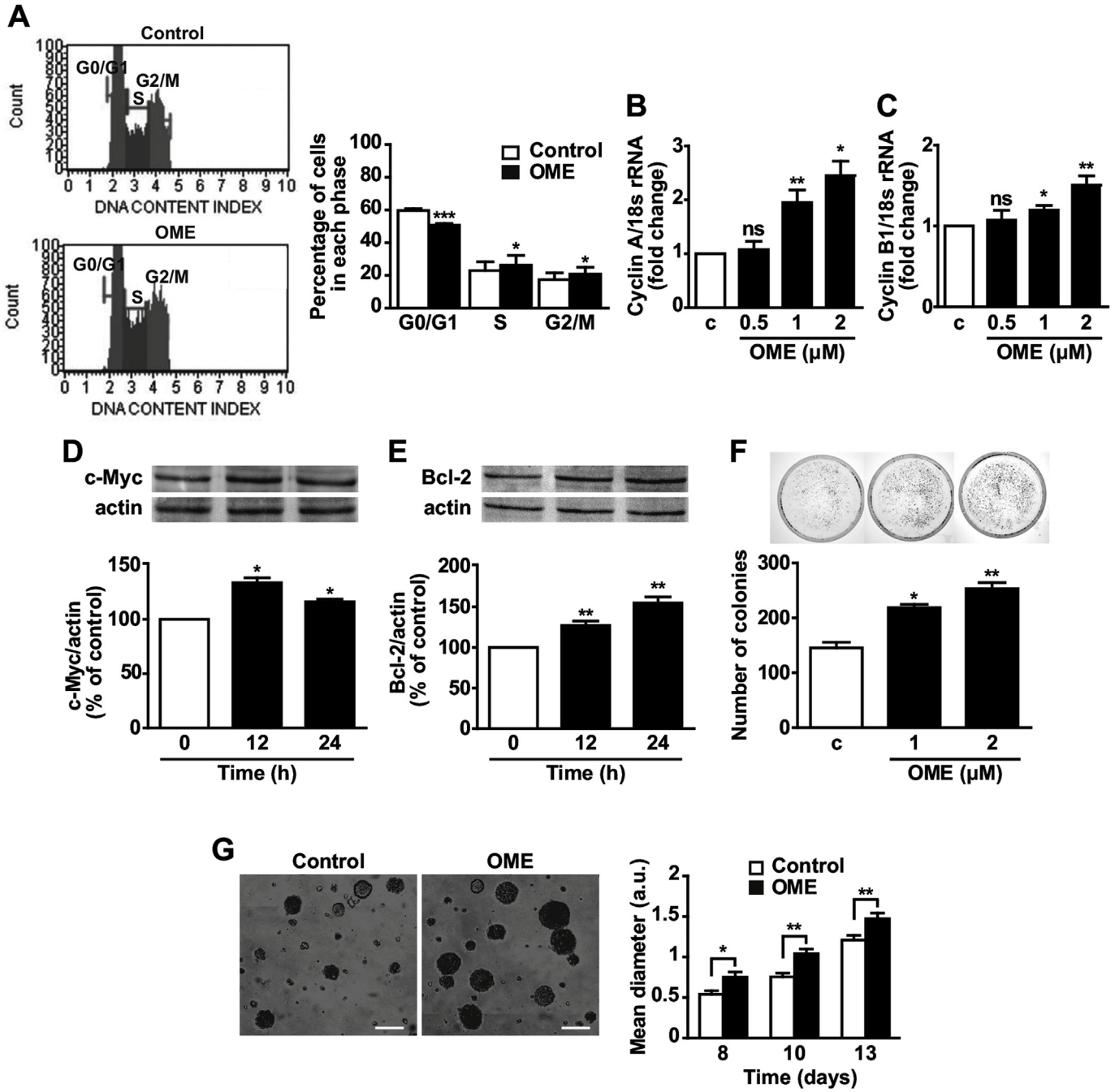

Fig. 3. Role of OME in regulation of cell cycle and formation of colonies and spheres in LNCaP cells. A, Distribution of cells in G0/G1, S and G2/M phases assessed by Muse™ Cell Cycle kit and analyzed by flow cytometry in cells treated for 24 h with 1 μM OME. Results are means ± SEM of three independent experiments. *$P < 0.05$ and ***$P < 0.001$ vs. Control in each phase. Real-time PCR for *cyclin A* (B) and *cyclin B1* (C) expression normalized to 18S rRNA in cells treated for 24 h with 1 μM OME. Results are the mean ± SEM of three independent experiments, each performed in triplicate. *$P < 0.05$ and **$P < 0.01$ vs. control (c); ns, not significant. D and E, Representative Western blot for c-Myc and Bcl-2 expression in cells treated for the times indicated with 1 μM OME. Results normalized to actin are expressed as percent of time 0 and are the mean ± SEM. *$P < 0.05$ and **$P < 0.01$ vs. Time 0 (n = 3). F, Colony formation in cells treated for 10 days either without or with OME, at the indicated concentrations. Results are the mean ± SEM. *$P < 0.05$ and **$P < 0.01$ vs. control (n = 3). G, Formation of spheres in cells cultured in Matrigel for the days indicated, in both absence or presence of 1 μM OME. Results are the mean ± SEM. *$P < 0.05$ and **$P < 0.01$ vs. control at each time point (n = 3). Scale bar: 100 μm.

an androgen-independent manner [37]. Along with cMyc, we observed an increase in Bcl-2 antiapoptotic protein, which is upregulated by PI3K/Akt and associated with prostate carcinogenesis and development of CRPC [38]. In agreement with these findings, OME also increased the number of colonies and the diameters of the spheres, further confirming the proliferative effect of PPIs and their potential ability to promote 3-dimensional (3D) anchorage-independent growth, one of the hallmarks of cell transformation and tumorigenic potential [2].

Importantly, although the mRNA levels of *AR* were unchanged, treatment with OME in LNCaP cells enhanced the phosphorylation of ErbB-2 and secretion of PSA, suggesting transactivation of AR. Accordingly, ErbB-2, whose intrinsic tyrosine kinase activity is constitutively increased in many types of cancer, has been shown to activate AR signaling in the absence of the ligand and to enhance the

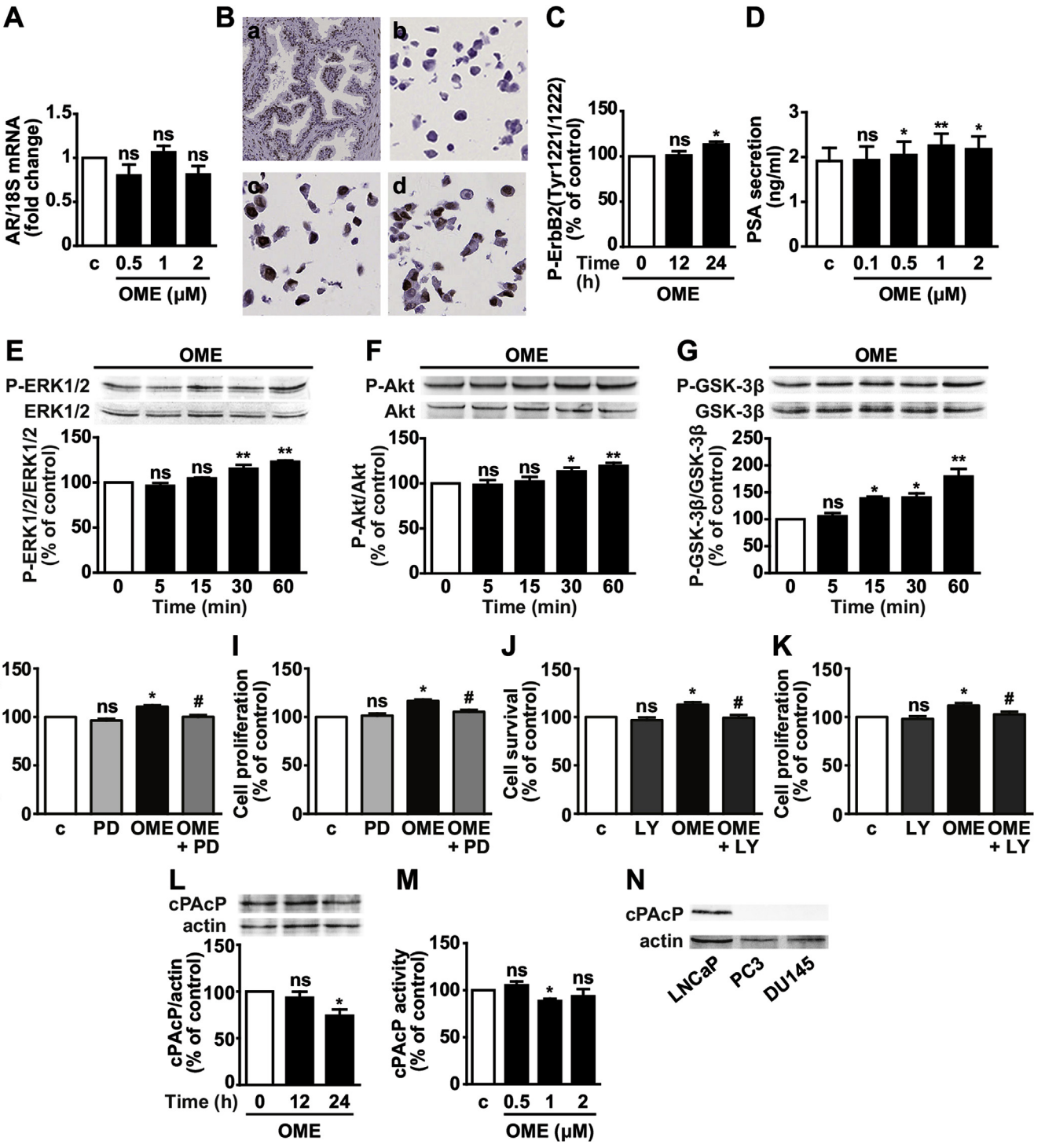

(caption on next page)

progression to androgen-independent PCa even in hormone-poor environment [39,40]. Moreover, ErbB-2 transactivates AR signaling in LNCaP cells through the MAPK pathway and elevation of PSA, a mechanism involved in CRPC [4]. ErbB-2 also promotes PCa cell growth in the absence of androgen through activation of Akt, phosphorylation of AR at Ser^{213} and Ser^{791} and elevation of the promoter activity of PSA gene [41]. In agreement with these observations, herein we show that along with ErbB-2, OME increased PSA secretion and phosphorylation of MAPK-ERK1/2, Akt and its downstream effector GSK-3β in LNCaP cells. Interestingly, inhibition of ERK1/2 and PI3K/Akt blunted the survival and proliferative effects of OME, suggesting that these pathways are implicated in the tumorigenic activities of the compound and its derivatives. Accordingly, studies have shown that MAPK-ERK1/2 and Akt/mammalian target of rapamycin (mTOR) signaling are often coordinately deregulated in human PCa and associated with progression to CRPC [3,42,43]. Furthermore, in mice, loss of the phosphatase and tensin homolog (PTEN) gene, which negatively regulates PI3K/Akt, results in activation of PI3K/Akt/mTOR and ERK1/2 in androgen-independent PCa [44]. Consistent with our results, inhibition of GSK-3β activity through phosphorylation of its upstream regulator Akt at Ser9 results in suppression of malignant PCa cell phenotype [45]; moreover, GSK-3β inhibitors attenuated PCa growth and mestastatic potential *in*

Fig. 4. Signaling pathways involved in the effects of OME in LNCaP cells. A, Real-time PCR for AR mRNA in LNCaP cells treated for 24 h with OME, at the concentrations indicated. Results, expressed as fold change of control, are mean ± SEM of three independent experiments, each performed in triplicate (ns, not significant). B, Representative immunoreactivity of AR protein in LNCaP cells untreated or treated for 24 h with 1 μM OME. a, normal prostate tissue (positive control); b, LNCaP cells incubated for 24 h without the antibody for AR (negative control); c and d, LNCaP cells untreated (c) or treated for 24 h with 1 μM OME (d). Original magnification, X 20. C, Tyrosine phosphorylation (Tyr1221/1222) of ErbB2 assessed by ELISA in cells treated with 1 μM OME for the times indicated. Results, expressed as percent of control, are mean ± SEM of three independent experiments performed in triplicate. *$P < 0.05$ vs. time 0. D, Secretion of PSA from cells treated for 24 h with OME, at the concentrations indicated. For both C and D, results are mean ± SEM of at least three independent experiments performed in triplicate. *$P < 0.05$ and **$P < 0.01$ vs. time 0 or control (c), respectively. E-G, Phosphorylation of ERK1/2 (E), Akt (F) and GSK-3β (G) in total lysates from cells cultured with 1 μM OME for the times indicated (top panels). Blots, each representative of three independent experiments, were reprobed with total antibodies for normalization (bottom panels). Graphs show phosphorylated proteins normalized to total proteins and reported as percentage of basal. *$P < 0.05$ and **$P < 0.01$ vs. time 0; ns, not significant. Cell survival (MTT assay) and proliferation (BrdU assay) in cells pretreated for 30 min with either PD98059 (40 μM) (H and I) or LY294002 (10 μM) (J and K), then treated for 24 h with 1 μM OME. *$P < 0.05$ vs. control (c); $^{\#}P < 0.05$ vs. OME (n = 3). L Expression of cPAcP protein assessed by Western blot in cells cultured with 1 μM OME for the times indicated (top panel). Equal protein loading was determined by reprobing with antibodies to actin (bottom panel). Graph shows the densitometric analysis of cPAcP normalized to actin and expressed as percent of time 0. *$P < 0.05$ vs. time 0 (n = 3). M cPAcP activity assessed by colorimetric enzymatic assay in cells either untreated or treated for 24 h with OME at the concentrations indicated. Results, expressed as percent of control are mean ± SEM. *$P < 0.05$ vs. control (c). N Expression of cPAcP in LNCaP, PC3 and DU145 cells assessed by Western blot (top panel). Blots were reprobed with antibody to actin for normalization (bottom panel) (n = 3).

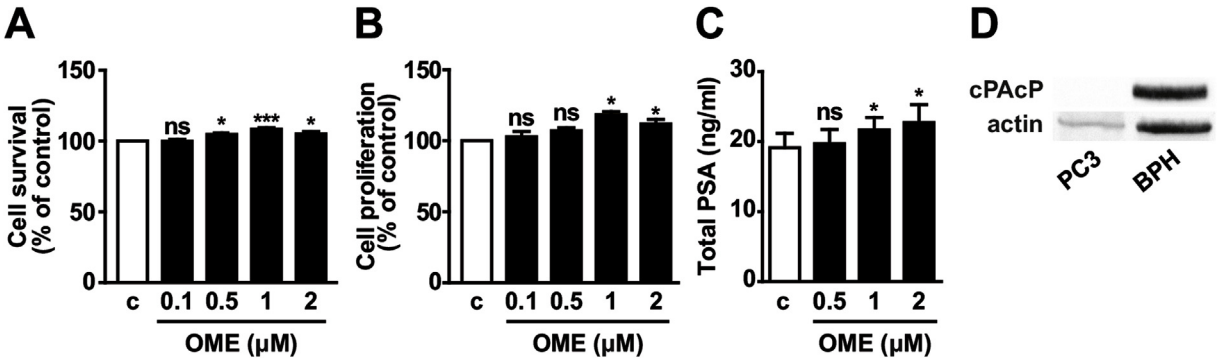

Fig. 5. Effect of OME on survival and proliferation of BPH cells. Serum-starved cells were cultured for 24 h with OME, at the concentrations indicated. Cell survival **(A)** and proliferation **(B)** were assessed by MTT and BrdU, respectively. Results, expressed as percent of control, are the mean ± SEM of three replicates (n = 3). *$P < 0.05$ vs. c; ns, not significant. **D** Expression of cPAcP in PC3 and BPH cells assessed by Western blot (top panel). Blots, representative of three independent experiments, were reprobed with antibody to actin for normalization (bottom panel).

vivo [46,47].

Our study reports that in LNCaP cells OME also reduced the expression and activity of the tyrosine phosphatase cPAcP, which was previously found to inhibit the growth of PCa cells in part through the dephosphorylation of ErbB-2 [31–33]. In fact, ErbB-2 is negatively associated with cPAcP activity, and the reduction of cPAcP has been associated with increased phosphorylation of ERK1/2, suggesting that inhibition of cPAcP results in activation of ErbB-2 and MAPK signaling [28]. Interestingly, studies have shown that expression and activity of cPAcP are lower in PCa cells than in normal and hypertrophic prostate tissue, and expression levels of cPAcP inversely correlate with PCa cell growth [31,32]. Accordingly, along with OME-induced inhibition of cPAcP, we showed expression of cPAcP protein in LNCaP but not in PC3 and DU145 cells, which have higher proliferation rate than LNCaP, suggesting that the molecular mechanisms involved in the effects of OME may be at least in part associated to inhibition of cPAcP. Furthermore, apart from LNCaP and BPH cells, OME, as well as LAN and ESO, showed little effect in DU145 and no effect in PC3 cells, which are both androgen-insensitive and negative for cPAcP expression [32]. Thus, based on the foregoing, our findings suggest that the survival and proliferative effects of OME in LNCaP cells involve transactivation of AR through mechanisms mediated by ErbB-2, MAPK-ERK1/2, Akt/GSK-3β signaling and inhibition of cPAcP.

Importantly, in addition to the effects in PCa cell lines, OME also increased the survival and proliferation, as well as PSA levels, in epithelial cells from BPH. Like LNCaP, BPH cells express cPAcP and previous studies have shown up-regulation of AR in BPH tissue, unveiling a potential role of AR in the etiopathogenesis of BPH [48]. Thus, it cannot be excluded that OME activates the same pathways in both LNCaP and BPH cells, although further studies are needed to verify this hypothesis.

Our results *in vitro* were confirmed *in vivo*, where treatment with a low dose of OME by oral gavage increased tumor progression and growth, and expression of PSA in mice xenografted with LNCaP cells. Accordingly, Huang et al. recently showed that long-term gavage with both low and high doses of OME promoted carcinogenesis of the mouse fore-stomach after treatment with nitrosamine, whereas no effect was observed with OME alone [16]. The mechanisms included the down-regulation of the cell cycle regulators p21 and mTOR. Interestingly, it has been previously shown that ESO reduces mTOR signaling in melanoma cell lines and promotes autophagy as a survival mechanism to counteract cell death [49]. Furthermore, co-administration of high doses of OME by oral gavage and β-naphtoflavone (BNF) in diet, promoted liver tumor in rats subjected to partial hepatectomy, but not liver initiation, through increased expression of cyclooxygenase 2 (COX-2) and cMyc [15]. Long-term administration of PPIs also worsened atrophic corpus gastritis and promoted adenocarcinoma development in Mongolian gerbils infected with Helicobacter pylori, although, differently from this study, OME was given with diet and at high dose [17]. However, the mechanisms involved in the above-mentioned studies are not fully explained and the direct role of PPIs in cancer cell growth remains to be studied in depth. In humans, long-term use of PPIs has been associated with increased risks of fundic gland polyps and gastric carcinoma [11–13], colorectal cancer [13] and pancreatic cancer [14] likely because of hypergastrinemia, which might increase the incidence of colorectal and gastric tumors [50]. Furthermore, although at present there are no data demonstrating the direct association between PPIs and PCa, it has been shown that CGA levels are increased in men after both short-and long-term use of PPIs [19,20]. Importantly, a recent study suggested a negative association between elevated levels of serum CGA and overall survival in men with metastatic CRPC [22].

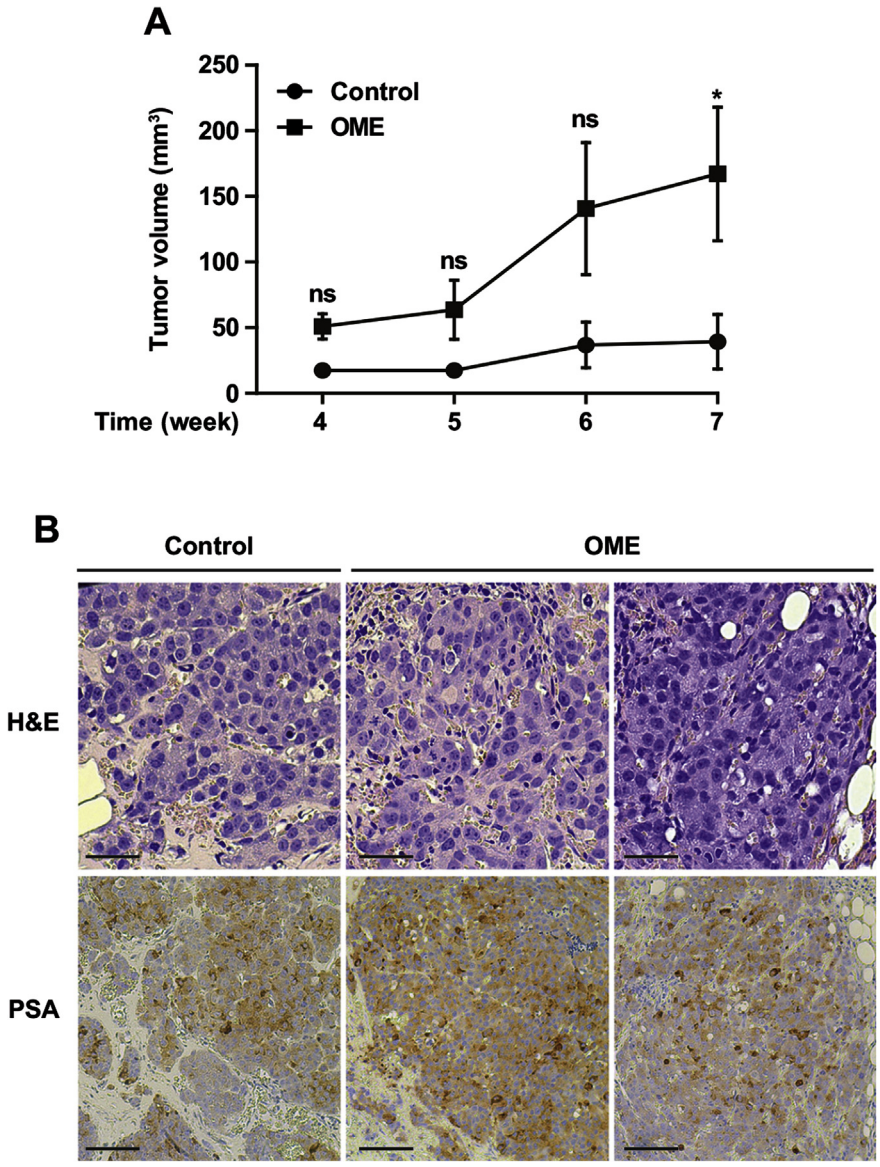

Fig. 6. ***In vivo*** **effect of OME in NOD/SCID mice bearing LNCaP xenografts**. **A** Tumor volume measured in LNCaP xenografts after treatment with either vehicle (Control) or OME (7.2 mg/kg), administered orally every two days for 7 weeks. Results are the mean ± SEM. $^{**}P < 0.01$ vs. Control; ns, not significant (n = 6 for each group). **B** Representative hematoxylin and eosin (H&E) staining (top panels), and immunoreactivity for PSA (bottom panels) in tumor tissues of control mice (left panels) and in mice treated with OME (middle and right panels) (Scale bar, 100 μm).

However, it has been also reported that LNCAP cells do not express CGA [51]; therefore, it is unlikely that the effects of OME in these cells are associated with an increase in CGA. New studies will be required to unveil the role of PPIs in CRPC cells.

In conclusion, we demonstrate that OME elicits survival and proliferative effects in PCa cell lines and primary BPH cell, and promote the growth of PCa in mice bearing LNCaP xenografts. The underlying mechanisms included the progression of cell cycle, increase in oncoproteins and reduction in antiapoptotic proteins, activation of proliferative pathways, along with elevation in PSA secretion and inhibition of prostate phosphatases. Therefore, our results suggest that PPIs may influence prostate carcinogenesis and/or progression to CRPC; however, additional studies are necessary to verify the potential long-term impact of these compounds in the development or progression of PCa in men. If confirmed in future research, these findings should be considered in the face of the broad use of PPIs, particularly when the therapeutic indication is weak.

Conflicts of interest

The authors declare no potential conflicts of interest.

Funding details

This work was supported by the Italian Ministry of Instruction and Research (PRIN 2015ZHKFTA_008 to E.G.) and Associazione Italiana per la Ricerca sul Cancro (AIRC; IG 18675 to L.P.).

Acknowledgments

We thank Prof. Dario Fontana for the critical suggestions and support.

Appendix A. Supplementary data

Supplementary data to this article can be found online at https://doi.org/10.1016/j.canlet.2019.02.028.

References

[1] R.L. Siegel, K.D. Miller, A. Jemal, Cancer statistics, 2018, CA Cancer J Clin 68 (2018) 7–30.
[2] M.M. Shen, C. Abate-Shen, Molecular genetics of prostate cancer: new prospects for old challenges, Genes Dev. 24 (2010) 1967–2000.
[3] D.E. Spratt, Z.S. Zumsteg, F.Y. Feng, S.A. Tomlins, Translational and clinical implications of the genetic landscape of prostate cancer, Nat. Rev. Clin. Oncol. 13 (2016) 597–610.
[4] S. Yeh, H.K. Lin, H.Y. Kang, T.H. Thin, M.F. Lin, C. Chang, From HER2/Neu signal cascade to androgen receptor and its coactivators: a novel pathway by induction of androgen target genes through MAP kinase in prostate cancer cells, Proc. Natl. Acad. Sci. U. S. A. 96 (1999) 5458–5463.
[5] E.C. Klinkenberg-Knol, F. Nelis, J. Dent, P. Snel, B. Mitchell, P. Prichard, D. Lloyd, N. Havu, M.H. Frame, J. Roman, A. Walan, Long-term omeprazole treatment in resistant gastroesophageal reflux disease: efficacy, safety, and influence on gastric mucosa, Gastroenterology 118 (2000) 661–669.
[6] P. Malfertheiner, A. Kandulski, M. Venerito, Proton-pump inhibitors: understanding the complications and risks, Nat. Rev. Gastroenterol. Hepatol. 14 (2017) 697–710.
[7] M.F. Vaezi, Y.X. Yang, C.W. Howden, Complications of proton pump inhibitor therapy, Gastroenterology 153 (2017) 35–48.
[8] A. Canitano, E. Iessi, E.P. Spugnini, C. Federici, S. Fais, Proton pump inhibitors induce a caspase-independent antitumor effect against human multiple myeloma, Cancer Lett. 376 (2016) 278–283.
[9] Y.Y. Lee, H.K. Jeon, J.E. Hong, Y.J. Cho, J.Y. Ryu, J.J. Choi, S.H. Lee, G. Yoon, W.Y. Kim, I.G. Do, M.K. Kim, T.J. Kim, C.H. Choi, J.W. Lee, D.S. Bae, B.G. Kim, Proton pump inhibitors enhance the effects of cytotoxic agents in chemoresistant epithelial ovarian carcinoma, Oncotarget 6 (2015) 35040–35050.
[10] K.S. Cheung, E.W. Chan, A.Y.S. Wong, L. Chen, I.C.K. Wong, W.K. Leung, Long-term proton pump inhibitors and risk of gastric cancer development after treatment for Helicobacter pylori: a population-based study, Gut 67 (2018) 28–35.
[11] A. Tran-Duy, B. Spaetgens, A.W. Hoes, N.J. de Wit, C.D. Stehouwer, Use of proton pump inhibitors and risks of fundic gland polyps and gastric cancer: systematic review and meta-analysis, Clin. Gastroenterol. Hepatol. 14 (2016) 1706–1719 e1705.
[12] N. Brusselaers, K. Wahlin, L. Engstrand, J. Lagergren, Maintenance therapy with proton pump inhibitors and risk of gastric cancer: a nationwide population-based cohort study in Sweden, BMJ Open 7 (2017) e017739.
[13] L.C. Soriano, M. Soriano-Gabarro, L.A. Garcia Rodriguez, Trends in the contemporary incidence of colorectal cancer and patient characteristics in the United Kingdom: a population-based cohort study using the Health Improvement Network, BMC Canc. 18 (2018) 402.
[14] M.D. Kearns, B. Boursi, Y.X. Yang, Proton pump inhibitors on pancreatic cancer risk and survival, Cancer Epidemiol. 46 (2017) 80–84.
[15] H. Hayashi, E. Taniai, R. Morita, M. Hayashi, D. Nakamura, A. Wakita, K. Suzuki, M. Shibutani, K. Mitsumori, Enhanced liver tumor promotion but not liver initiation activity in rats subjected to combined administration of omeprazole and beta-naphthoflavone, J. Toxicol. Sci. 37 (2012) 969–985.
[16] L. Huang, D.J. Qi, W. He, A.M. Xu, Omeprazole promotes carcinogenesis of forestomach in mice with co-stimulation of nitrosamine, Oncotarget 8 (2017) 70332–70344.
[17] T. Hagiwara, K. Mukaisho, T. Nakayama, H. Sugihara, T. Hattori, Long-term proton pump inhibitor administration worsens atrophic corpus gastritis and promotes adenocarcinoma development in Mongolian gerbils infected with Helicobacter pylori, Gut 60 (2011) 624–630.
[18] J. von Hardenberg, M. Schwartz, T. Werner, S. Fuxius, M. Muller, C. Bolenz, C. Weiss, E. Heinrich, Influence of abiraterone acetate on circulating neuromediators in chemotherapy-naive castration-resistant prostate cancer, Prostate 76 (2016) 613–619.
[19] M. Giusti, M. Sidoti, C. Augeri, C. Rabitti, F. Minuto, Effect of short-term treatment with low dosages of the proton-pump inhibitor omeprazole on serum chromogranin A levels in man, Eur. J. Endocrinol. 150 (2004) 299–303.
[20] D. Raines, M. Chester, A.E. Diebold, P. Mamikunian, C.T. Anthony, G. Mamikunian, E.A. Woltering, A prospective evaluation of the effect of chronic proton pump inhibitor use on plasma biomarker levels in humans, Pancreas 41 (2012) 508–511.
[21] A.I. Vinik, E.A. Woltering, R.R. Warner, M. Caplin, T.M. O'Dorisio, G.A. Wiseman, D. Coppola, V.L. Go, S. North American Neuroendocrine Tumor, NANETS consensus guidelines for the diagnosis of neuroendocrine tumor, Pancreas 39 (2010) 713–734.
[22] K.V. Giridhar, C. Sanhueza, D.W. Hillman, H. Alkhateeb, R. Carlson, W. Tan, B.A. Costello, F. Quevedo, L. Pagliaro, M. Kohli, Serum chromogranin-A-based prognosis in metastatic castration-resistant prostate cancer, Prostate Cancer Prostatic Dis. 21 (3) (2018) 431–437.
[23] R. Granata, F. Settanni, L. Trovato, D. Gallo, I. Gesmundo, R. Nano, M.P. Gallo, L. Bergandi, M. Volante, G. Alloatti, L. Piemonti, J. Leprince, M. Papotti, H. Vaudry, H. Ong, E. Ghigo, RFamide peptides 43RFa and 26RFa both promote survival of pancreatic beta-cells and human pancreatic islets but exert opposite effects on insulin secretion, Diabetes 63 (2014) 2380–2393.
[24] I. Gesmundo, M. Miragoli, P. Carullo, L. Trovato, V. Larcher, E. Di Pasquale, M. Brancaccio, M. Mazzola, T. Villanova, M. Sorge, M. Taliano, M.P. Gallo, G. Alloatti, C. Penna, J.M. Hare, E. Ghigo, A.V. Schally, G. Condorelli, R. Granata, Growth hormone-releasing hormone attenuates cardiac hypertrophy and improves heart function in pressure overload-induced heart failure, Proc. Natl. Acad. Sci. U. S. A. 114 (2017) 12033–12038.
[25] E. Gargantini, L. Lazzari, F. Settanni, M. Taliano, L. Trovato, I. Gesmundo, E. Ghigo, R. Granata, Obestatin promotes proliferation and survival of adult hippocampal progenitors and reduces amyloid-beta-induced toxicity, Mol. Cell. Endocrinol. 422 (2016) 18–30.
[26] A. Puliafito, A. De Simone, G. Seano, P.A. Gagliardi, L. Di Blasio, F. Chianale, A. Gamba, L. Primo, A. Celani, Three-dimensional chemotaxis-driven aggregation of tumor cells, Sci. Rep. 5 (2015) 15205.
[27] D.I. Quinn, H.M. Sandler, L.G. Horvath, A. Goldkorn, J.A. Eastham, The evolution of chemotherapy for the treatment of prostate cancer, Ann. Oncol. 28 (2017) 2658–2669.
[28] M.S. Lee, T. Igawa, T.C. Yuan, X.Q. Zhang, F.F. Lin, M.F. Lin, ErbB-2 signaling is involved in regulating PSA secretion in androgen-independent human prostate cancer LNCaP C-81 cells, Oncogene 22 (2003) 781–796.
[29] S. Hatakeyama, T. Yoneyama, Y. Tobisawa, C. Ohyama, Recent progress and perspectives on prostate cancer biomarkers, Int. J. Clin. Oncol. 22 (2017) 214–221.
[30] D.J. Mulholland, S. Dedhar, H. Wu, C.C. Nelson, PTEN and GSK3beta: key regulators of progression to androgen-independent prostate cancer, Oncogene 25 (2006) 329–337.
[31] S. Muniyan, M.A. Ingersoll, S.K. Batra, M.F. Lin, Cellular prostatic acid phosphatase, a PTEN-functional homologue in prostate epithelia, functions as a prostate-specific tumor suppressor, Biochim. Biophys. Acta 1846 (2014) 88–98.
[32] M.F. Lin, M.S. Lee, X.W. Zhou, J.C. Andressen, T.C. Meng, S.L. Johansson, W.W. West, R.J. Taylor, J.R. Anderson, F.F. Lin, Decreased expression of cellular prostatic acid phosphatase increases tumorigenicity of human prostate cancer cells, J. Urol. 166 (2001) 1943–1950.
[33] T.D. Chuang, S.J. Chen, F.F. Lin, S. Veeramani, S. Kumar, S.K. Batra, Y. Tu, M.F. Lin, Human prostatic acid phosphatase, an authentic tyrosine phosphatase, dephosphorylates ErbB-2 and regulates prostate cancer cell growth, J. Biol. Chem. 285 (2010) 23598–23606.
[34] M.F. Lin, J. DaVolio, R. Garcia-Arenas, Expression of human prostatic acid phosphatase activity and the growth of prostate carcinoma cells, Cancer Res. 52 (1992) 4600–4607.
[35] A. Kahokehr, P.J. Gilling, Landmarks in BPH–from aetiology to medical and surgical management, Nat. Rev. Urol. 11 (2014) 118–122.
[36] T.K. Fung, H.T. Ma, R.Y. Poon, Specialized roles of the two mitotic cyclins in somatic cells: cyclin A as an activator of M phase-promoting factor, Mol. Biol. Cell 18 (2007) 1861–1873.
[37] D. Bernard, A. Pourtier-Manzanedo, J. Gil, D.H. Beach, Myc confers androgen-independent prostate cancer cell growth, J. Clin. Invest. 112 (2003) 1724–1731.
[38] S.D. Catz, J.L. Johnson, BCL-2 in prostate cancer: a minireview, Apoptosis 8 (2003) 29–37.
[39] N. Craft, Y. Shostak, M. Carey, C.L. Sawyers, A mechanism for hormone-independent prostate cancer through modulation of androgen receptor signaling by the HER-2/neu tyrosine kinase, Nat. Med. 5 (1999) 280–285.
[40] Y. Yarden, G. Pines, The ERBB network: at last, cancer therapy meets systems biology, Nat. Rev. Canc. 12 (2012) 553–563.
[41] Y. Wen, M.C. Hu, K. Makino, B. Spohn, G. Bartholomeusz, D.H. Yan, M.C. Hung, HER-2/neu promotes androgen-independent survival and growth of prostate cancer cells through the Akt pathway, Cancer Res. 60 (2000) 6841–6845.
[42] D. Gioeli, J.W. Mandell, G.R. Petroni, H.F. Frierson Jr., M.J. Weber, Activation of mitogen-activated protein kinase associated with prostate cancer progression, Cancer Res. 59 (1999) 279–284.
[43] S.N. Malik, M. Brattain, P.M. Ghosh, D.A. Troyer, T. Prihoda, R. Bedolla, J.I. Kreisberg, Immunohistochemical demonstration of phospho-Akt in high Gleason grade prostate cancer, Clin. Cancer Res. 8 (2002) 1168–1171.
[44] H. Gao, X. Ouyang, W.A. Banach-Petrosky, W.L. Gerald, M.M. Shen, C. Abate-Shen, Combinatorial activities of Akt and B-Raf/Erk signaling in a mouse model of androgen-independent prostate cancer, Proc. Natl. Acad. Sci. U. S. A. 103 (2006) 14477–14482.
[45] A. Wei, B. Fan, Y. Zhao, H. Zhang, L. Wang, X. Yu, Q. Yuan, D. Yang, S. Wang, ST6Gal-I overexpression facilitates prostate cancer progression via the PI3K/Akt/GSK-3beta/beta-catenin signaling pathway, Oncotarget 7 (2016) 65374–65388.
[46] Q. Zhu, J. Yang, S. Han, J. Liu, J. Holzbeierlein, J.B. Thrasher, B. Li, Suppression of glycogen synthase kinase 3 activity reduces tumor growth of prostate cancer in vivo, Prostate 71 (2011) 835–845.
[47] J. Kroon, L.S. in 't Veld, J.T. Buijs, H. Cheung, G. van der Horst, G. van der Pluijm, Glycogen synthase kinase-3beta inhibition depletes the population of prostate cancer stem/progenitor-like cells and attenuates metastatic growth, Oncotarget 5 (2014) 8986–8994.
[48] K. Izumi, A. Mizokami, W.J. Lin, K.P. Lai, C. Chang, Androgen receptor roles in the development of benign prostate hyperplasia, Am. J. Pathol. 182 (2013) 1942–1949.
[49] M.L. Marino, S. Fais, M. Djavaheri-Mergny, A. Villa, S. Meschini, F. Lozupone, G. Venturi, P. Della Mina, S. Pattingre, L. Rivoltini, P. Codogno, A. De Milito, Proton pump inhibition induces autophagy as a survival mechanism following oxidative stress in human melanoma cells, Cell Death Dis. 1 (2010) e87.
[50] R. Dawson, J.M. Manson, Omeprazole in oesophageal reflux disease, Lancet 356 (2000) 1770–1771.
[51] A. Leiblich, S.S. Cross, J.W. Catto, G. Pesce, F.C. Hamdy, I. Rehman, Human prostate cancer cells express neuroendocrine cell markers PGP 9.5 and chromogranin A, Prostate 67 (2007) 1761–1769.